[3Fe–4S] to [4Fe–4S] Cluster Conversion in *Escherichia coli* Fumarate Reductase by Site-Directed Mutagenesis†

Annamaria Manodori,‡ Gary Cecchini,‡ Imke Schröder,§ Robert P. Gunsalus,§ Mark T. Werth,∥ and Michael K. Johnson*,∥

Molecular Biology Division, Veterans Administration Medical Center, San Francisco, California 94121, Department of Biochemistry and Biophysics, University of California, San Francisco, California 94143, Department of Microbiology and Molecular Genetics and Molecular Biology Institute, University of California, Los Angeles, California 90024, and Department of Chemistry and Center for Metalloenzyme Studies, University of Georgia, Athens, Georgia 30602

Received October 30, 1991; Revised Manuscript Received December 30, 1991

ABSTRACT: Site-directed mutants of *Escherichia coli* fumarate reductase in which FrdB Cys^{204}, Cys^{210}, and Cys^{214} were individually replaced by Ser and in which Val^{207} was replaced by Cys were constructed and overexpressed in a strain of *E. coli* lacking a wild-type copy of fumarate reductase and succinate dehydrogenase. The consequences of these mutations on bacterial growth, enzymatic activity, and the EPR properties of the constituent iron–sulfur clusters were investigated. The FrdB Cys^{204}Ser, Cys^{210}Ser, and Cys^{214}Ser mutations result in enzymes with negligible activity that have dissociated from the membrane and consequently are incapable of supporting cell growth under conditions requiring a functional fumarate reductase. EPR studies indicate that these effects are associated with loss of both the [3Fe–4S] and [4Fe–4S] clusters, centers 3 and 2, respectively. In contrast, the FrdB Val^{207}Cys mutation results in a functional membrane-bound enzyme that is able to support growth under anaerobic and aerobic conditions. However, EPR studies indicate that the indigenous $[3Fe–4S]^{+,0}$ cluster (E_m = −70 mV), center 3, has been replaced by a much lower potential $[4Fe–4S]^{2+,+}$ cluster (E_m = −350 mV), indicating that the primary sequence of the polypeptide determines the type of clusters assembled. The results of these studies afford new insights into the role of centers 2 and 3 in mediating electron transfer from menaquinol, the residues that ligate these clusters, and the intercluster magnetic interactions in the wild-type enzyme.

Fumarate reductase (menaquinol–fumarate oxidoreductase) from *Escherichia coli* is a four-subunit membrane-bound complex that is produced during anaerobic growth with fumarate as the terminal electron acceptor (Kröger, 1978; Ingledew & Poole, 1984). The membrane-extrinsic catalytic domain consists of a flavoprotein (Fp),[1] FrdA (66 kDa) with a covalently bound FAD (Weiner & Dickie, 1979), and an iron–sulfur protein (Ip), FrdB (27 kDa). Two smaller hydrophobic polypeptides FrdC and FrdD (15 and 13 kDa) serve to anchor the complex to the membrane and provide sites for the enzyme to interact with quinones (Lemire et al., 1982; Cecchini et al., 1986a). The enzyme has three distinct types of iron–sulfur clusters: center 1, $[2Fe–2S]^{2+,+}$ (E_m = −20 to −79 mV); center 2, $[4Fe–4S]^{2+,+}$ (E_m = −320 mV); and center 3, $[3Fe–4S]^{+,0}$ (E_m = −70 mV) (Morningstar et al., 1985; Johnson et al., 1985c,d; Cammack et al., 1986b; Werth et al., 1990). The physical and catalytic properties of the fumarate reductase complex (FrdABCD) are very similar to those of succinate–ubiquinone oxidoreductase (complex II) from mitochondria and bacteria (Ohnishi, 1987; Cole et al., 1985; Ackrell et al., 1991). Furthermore, *E. coli* fumarate reductase will catalyze succinate oxidation at 30–40% of the rate at which it reduces fumarate (Cecchini et al., 1986a), and the *frd* gene products will replace succinate dehydrogenase in *sdh* mutants when produced from multicopy plasmids (Guest, 1981). These properties make *E. coli* fumarate reductase an excellent model system for studies of both enzyme systems and their prosthetic groups. Questions remain concerning the assembly, location, and ligation of the Fe–S clusters and their involvement in electron transfer from menaquinol to fumarate.

The Ip subunits of all fumarate reductases and succinate dehydrogenases sequenced to date show a high degree of homology with the cysteine residues conserved in three ferredoxin-like clusters (Cole et al., 1982; Darlison & Guest, 1984; Yao et al., 1986; Phillips et al., 1987; Lauterbach et al., 1990). Recent site-directed mutagenesis experiments in which each of the first group of four cysteines in *E. coli* fumarate reductase (Cys^{57}, Cys^{62}, Cys^{65}, and Cys^{77}) were individually mutated to serines demonstrates the involvement of these residues in ligating the [2Fe–2S] cluster, center 1 (Werth et al., 1990). In Figure 1 the arrangement of the highly conserved second and third groups of cysteinyl residues in fumarate reductases and succinate dehydrogenases is compared to the arrangements of cysteinyl residues ligating [4Fe–4S] and [3Fe–4S] clusters in bacterial ferredoxins. By analogy to structurally characterized ferredoxins, it is logical to assign the first three cysteines of the second group and the last cysteine of the third group (Cys^{148}, Cys^{151}, Cys^{154}, and Cys^{214} in *E. coli* FrdB) as ligands of the [4Fe–4S] cluster, center 2,

† This work was supported by the Veterans Administration and grants from the National Science Foundation (DMB9104297 to G.C.), the National Institutes of Health (HL16251 to G.C. and R.P.G. and GM33806 to M.K.J.), and the Deutche Forschungsgemeinschaft (to I.S.).

* Address correspondence to this author at the Department of Chemistry, University of Georgia, Athens, GA 30602.

‡ Molecular Biology Division, Veterans Administration Medical Center, San Francisco, and Department of Biochemistry and Biophysics, University of California at San Francisco.

§ Department of Microbiology and Molecular Genetics and Molecular Biology institute, University of California at Los Angeles.

∥ Department of Chemistry and Center for Metalloenzyme Studies, University of Georgia.

[1] Abbreviations: Fp, flavoprotein; Ip, iron–sulfur protein; PMS, phenazine methosulfate; BV_{red}, reduced benzyl viologen; Q, quinone; MQH_2, menaquinol-6; DPB, 2,3-dimethoxy-5-methyl-6-pentyl-1,4-benzoquinone.

0006-2960/92/0431-2703$03.00/0

Table I: *E. coli* Strains, Plasmids, and Phage

strain	origin	genotype	source
bacteria			
DW35	MC4100	F⁻ zjd::Tn10 Δ(*frdABCD*)18 *sdhC*::*kan ara*D139 Δ(*argF–lac*) *U*169 *rpsL*150 *rel*A1 *flb*B5301 *deo*C1 *pfs*F25 *rbs*R	*a*
DH5α		F⁻ φ80d/*lac*ZΔM15 *end*A1 *rec*A1 *hsd*R17(r_{k-},m_{k+}) *sup*E44 *thi*-1 *gyr*A *rel*A1 Δ(*lac*ZYA–*arg*F) *U*169 λ⁻	*b*
CJ236		*dut ung thi relA* pCJ105 (*Cm*^{r})	*c*
MV1190		(Δ*lac–pro* AB)*thi sup*E Δ(*srl–recA*)306::Tn10(*tet*^{r}) [F′:*tra*D36 *pro*AB *lac*I^{q}ZΔM15]	*d*
plasmids			
pH3	pBR322	*frd*A$^+$B$^+$C$^+$D$^+$	*e*
pH3FrdBV^{207}C	pH3	*frd*A$^+$B^{V207C}C$^+$D$^+$	this study
pH3FrdBC^{204}S	pH3	*frd*A$^+$B^{C204S}C$^+$D$^+$	this study
pH3FrdBC^{210}S	pH3	*frd*A$^+$B^{C210S}C$^+$D$^+$	this study
pH3FrdBC^{214}S	pH3	*frd*A$^+$B^{C214S}C$^+$D$^+$	this study
pFRD23	pACYC184	*frd*A$^+$B$^+$	*f*
phage			
M13mp8			*g*
M13KW1	M13mp8	*frd*B$^+$(ΔACD)	*h*

[a] Schröder et al. (1991). [b] Hannahan (1983). [c] Joyce and Grindley (1984). [d] Bio-Rad "MUTA-GENE M13 in vitro mutagenesis kit", Bio-Rad Laboratories, Richmond, CA. [e] Blaut et al. (1989). [f] Cecchini et al. (1986). [g] Messing and Vieira (1982). [h] Werth et al. (1990).

E. coli	FrdIp	147	G C I N C G L C Y A A C P Q F	161
W. succinogenes	FrdIp	149	R C I E C G C C I A A C G T K	163
Beef Heart	SdhIp	157	E C I L C A C C S T S C P S Y	171
B. subtilis	SdhIp	153	K C M T C G V C L E A C P N V	167
E. coli	SdhIp	147	E C I L C A C C S T S C P S F	161
P. aerogenes	8Fe Fd	7	S C I A C G A C K P E C P V N	21
T. thermophilus	7Fe Fd	38	E C I D C G A C K P E C P V N	52
A. vinelandii	7Fe FdI	38	E C I D C A L C E P E C P A E	52

E. coli	FrdIp	203	S C T F V G - - Y C S E V C P	215
W. succinogenes	FrdIp	206	G C M T L L - - A C H D V C P	218
Beef Heart	SdhIp	214	R C H T I M - - N C T E T C P	226
B. subtilis	SdhIp	210	D C G N S Q - - N C V Q S C P	222
E. coli	SdhIp	204	R C H S I M - - N C V S V C P	216
P. aerogenes	8Fe Fd	34	S C I D C G - - S C A S V C P	46
T. thermophilus	7Fe Fd	7	P C I G V K D Q S C V E V C P	21
A. vinelandii	7Fe FdI	7	N C I K C K Y T D C V E V C P	21

FIGURE 1: Comparison of the arrangement of cysteine residues in the Ip subunits of fumarate reductase (Frd) from *E. coli* (Cole et al., 1982) and *Wolinella succinogenes* (Lauterbach et al., 1990) and succinate dehydrogenase (Sdh) from beef heart (Yao et al., 1986), *Bacillus subtilis* (Phillips et al., 1987), and *E. coli* (Darlison & Guest, 1984) with those of the 8Fe-ferredoxin from *Peptococcus aerogenes* (now known as *Peptostreptococcus asaccharolyticus*) (Adman et al., 1973) and the 7Fe-ferredoxins from *Thermus thermophilus* (Sato et al., 1981) and *Azotobacter vinelandii* (Howard et al., 1983).

and the first two cysteines of the third group and the last cysteine of the second group (Cys^{157}, Cys^{204}, and Cys^{210} in *E. coli* FrdB) as ligands of the [3Fe–4S] cluster, center 3. The arrangement of cysteinyl residues thus assigned as ligands to the [3Fe–4S] cluster in fumarate reductases and succinate dehydrogenases is very similar to the consensus sequence for [4Fe–4S] clusters in bacterial ferredoxins (Cys–xx–Cys–xx–Cys and a remote Cys–Pro), except that the second cysteine ligand in the sequence is replaced by a neutral amino acid (Val^{207} in *E. coli* FrdB). Moreover, it is known from the X-ray structure of *Desulfovibrio gigas* ferredoxin II (Kissinger et al., 1988, 1989) and spectroscopic studies of ferredoxins from *Pyrococcus furiosus* (Conover et al., 1990) and *Desulfovibrio africanus* (George et al., 1989) that the second cysteine of the bacterial ferredoxin [4Fe–4S] consensus sequence is the one not required for ligation of a [3Fe–4S] cluster. Indeed it is now well established that facile [4Fe–4S] ↔ [3Fe–4S] cluster interconversions are often possible in bacterial ferredoxins provided a coordinating residue such as cysteine or aspartate occupies this position (Beinert & Thomson, 1983; George et al., 1989; Conover et al., 1990).

As part of ongoing studies to investigate the role of the iron–sulfur clusters of fumarate reductase in electron transport, we report on the enzymatic and structural consequences of site-directed Cys → Ser mutations involving each of the last three cysteines in *E. coli* FrdB (Cys^{204}, Cys^{210}, and Cys^{214}) and the construction and characterization of a mutant in which FrdB Val^{207} is replaced by a cysteine residue. The rationale for the FrdB Val^{207}Cys substitution was to determine if the primary amino acid sequence of FrdB encodes the information for insertion of a [3Fe–4S] cluster versus a [4Fe–4S] cluster. The results suggest that is indeed the case, and the resultant ability to alter the properties of center 3, while preserving the structural integrity of the enzyme complex, offers new insights into the intercluster spin–spin interactions and the roles of centers 2 and 3 in mediating electron transfer. In addition, the results address the question of the specific cysteine residues ligating centers 2 and 3 in the wild-type enzyme.

Materials and Methods

Strains, Plasmids, and Phage. The *E. coli* strains, plasmids, and phage used in this work are listed in Table I. Strain DW35 contains a deletion of *frdABCD* and a *kan* insertion in the *sdhCDAB* (*sdhC*::*kan*) region which causes a disruption of the operon (Schröder et al., 1991). Phage M13KW1 was constructed by inserting the 2.0-kilobase (kb) *Eco*R1–*Sal*I fragment from pH3 into the polylinker site of M13mp8 (Werth et al., 1990).

Site-Directed Mutagenesis. Site-directed mutagenesis was performed using the in vitro mutagenesis system from Bio-Rad (Richmond, CA) based on the method developed by Kunkel (Kunkel, 1985; Kunkel et al., 1987). Oligonucleotides for mutagenesis and sequencing were synthesized on a Biosearch model 8700. The oligonucleotides were designed to change FrdB Val^{207} to cysteine or Cys^{204}, Cys^{210}, and Cys^{214} to serine residues. The mutagenesis was performed using single-stranded M13KW1 DNA as a template. The mutants were identified by DNA sequence analysis using the dideoxy termination procedure (Sanger et al., 1977) and a Pharmacia sequencing kit. Strains CJ236 and MV190 supplied by Bio-Rad were used as hosts for mutagenesis and single-stranded DNA sequence analysis. Following mutagenesis, the 2.0-kb *Eco*RI–*Sal*I fragment containing the *frdB* region was cloned back into the large *Eco*RI–*Sal*I fragment of plasmid pH3 to restore the complete *frdABCD* operon. The plasmid was transformed into DH5α, and the construct was confirmed by double-stranded DNA sequencing. DNA was prepared using

Table II: Growth Properties and Catalytic Activities of *E. coli* DW35 with Amplified Expression of Wild-Type or Mutant Fumarate Reductase

encoded subunits	doubling time (h)			turnover number (min^{-1})[c]			
	$-O_2$[a]	$+O_2$[b]	FAD[f]	BV	MQ	PMS	DPB
FrdABCD (wild-type)	2.0	2.1	1.47	19000	6000	5300	2400
$FrdAB^{V207C}CD$	4.6	3.0	2.04	11000	1000	1600	390
$FrdAB^{C204S}CD$[d]	NG[e]	NG	0.04	140	0	130	15
$FrdAB^{C210S}CD$[d]	NG	NG	0.07	80	0	26	7
$FrdAB^{C214S}CD$[d]	NG	NG	0.10	55	0	40	12
FrdAB(ΔFrdCD)[d]	NG	NG	0.23	5500	0	3900	200

[a] $-O_2$, anaerobic growth on glycerol/fumarate minimal medium. [b] $+O_2$, aerobic growth in succinate minimal medium. [c] Turnover numbers represent an average of at least two determinations; BV, BV_{red} fumarate oxidoreductase activity; MQ, MQH_2 fumarate oxidoreductase activity; PMS, succinate PMS oxidoreductase activity; DPB, succinate DPB oxidoreductase activity. [d] Enzyme located in cytoplasmic fractions. [e] NG, no growth. [f] Covalent FAD, nmol/mg of protein. The center 1 EPR signal in dithionite-reduced samples of wild-type and mutant samples accounted for one spin/FAD within the combined experimental error of the FAD assays and EPR spin quantitations (±20%).

the Qiagen plasmid kit from Diagen (Chatsworth, CA).

Growth of Bacteria. For growth studies and biochemical analysis, the mutant plasmids were transformed into *E. coli* strain DW35 (Δ*frdABCD*, *sdhC*::*kan*). Wild-type and mutants were grown anaerobically on glycerol/fumarate or glucose/fumarate minimal media, or aerobically on minimal succinate media as peviously described (Schröder et al., 1991; Cecchini et al., 1986b). To prepare purified membrane fractions of the wild-type and $Val^{207}Cys$ mutant, cells were grown anaerobically on glycerol/fumarate medium to stationary phase, harvested by centrifugation, and frozen at −20 °C. Since the $Cys^{204}Ser$, $Cys^{210}Ser$, and $Cys^{214}Ser$ mutants are unable to grow under conditions requiring a functional fumarate reductase or succinate dehydrogenase, cells were grown on a glucose/fumarate medium. For phage and plasmid manipulations, cells were grown on Luria broth and solid media (Blaut et al., 1989).

Purification of Cellular Fractions Enriched in Fumarate Reductase. Sixty grams (wet weight) of *E. coli* DW35 containing the appropriate plasmid were suspended in 300 mL of 30 mM Tris-HCl (pH 8.0). The cytoplasmic-membrane/fumarate reductase fraction was then purified as previously described (Lemire & Weiner, 1986). Crude membrane and cytoplasmic fractions were prepared as described in Cecchini et al. (1986b).

Enzyme Assays. Enzyme activity assays were conducted as in previous work (Cecchini et al., 1986a,b) using reduced benzyl viologen (BV_{red}) and menaquinol-6 (MQH_2) as the electron donors for fumarate reduction. The oxidation of succinate was measured with phenazine methosulfate (PMS) and 2,3-dimethoxy-5-methyl-6-pentyl-1,4-benzoquinone (DPB) as primary electron acceptors. Enzyme concentration was determined as covalently bound histidyl-FAD using established procedures (Salach et al., 1972).

EPR Spectroscopy. Samples for EPR spectroscopy were prepared under an argon atmosphere in a Vacuum Atmospheres (Hawthorne, CA) glove box (<1 ppm O_2). Cytoplasmic-membrane preparations were resuspended in a minimal volume of 50 mM Tris-HCl buffer, pH 7.8. Fumarate-, succinate-, and dithionite-treated samples were prepared anaerobically by addition of 20 mM fumarate, 20 mM succinate, or 10 mM dithionite followed by incubation for 10 min at room temperature prior to freezing in liquid nitrogen. EPR redox titrations were performed at ambient temperature (25–27 °C) in the glove box using cytoplasmic-membrane preparations resuspended in anaerobic 100 mM potassium phosphate, pH 7.2. Mediator dyes were added, each to a concentration of ca. 50 μM, in order to cover the desired range of redox potentials, i.e., neutral red, safranin, phenosafranin, 2-hydroxy-1,4-anthraquinone, 2-hydroxy-1,4-naphthoquinone, indigodisulfonate, methylene blue, 1,4-naphthoquinone, and duroquinone. Methyl and benzyl viologen were omitted to avoid large radical signals centered at $g = 2$. Samples were first reduced completely by addition of excess sodium dithionite followed by oxidative titration with potassium ferricyanide. After equilibration at the desired potential, a 0.2-mL aliquot was transferred to a calibrated EPR tube and immediately frozen in liquid nitrogen. Potentials were measured with a platinum working electrode and a saturated calomel reference electrode. All redox potentials are reported relative to the standard hydrogen electrode.

X-band EPR spectra were recorded using an IBM/Bruker ER200D spectrometer interfaced to an ESP 1600 data processing system for data storage and manipulation. Low temperatures were obtained with an Oxford Instruments ESR-9 cryostat. Spin quantitations were obtained under nonsaturating conditions by double integration with reference to a 1 mM CuEDTA standard measured under identical conditions.

Results

The involvement of the last group of three cysteine residues in FrdB (Cys^{204}, Cys^{210}, and Cys^{214}) in ligating Fe–S clusters was assessed by site-directed mutation of each to a serine residue. In addition, the FrdB $Val^{207}Cys$ mutant was constructed to investigate the role of the [3Fe–4S] cluster in electron transfer and to determine if the amino acid sequence is the primary driving force controlling the insertion of a [3Fe–4S] versus a [4Fe–4S] cluster into FrdB. The mutagenized plasmid DNA was transformed into *E. coli* strain DW35 (Δ*frdABCD*, *sdhC*::*kan*) so that background of wild-type succinate dehydrogenase and fumarate reductase is eliminated from the subsequent enzymatic and spectroscopic analyses.

Growth Studies. To test whether the FrdB mutant enzymes were physiologically functional, we measured the doubling time of cells grown anaerobically on glycerol/fumarate medium or aerobically on minimal succinate medium (see Table II). Under these conditions a functional fumarate reductase is required, i.e., the deletion strain DW35 with no complementing plasmids does not grow in either of these media. Doubling times of cells carrying plasmids with wild-type fumarate reductase were 2.0 and 2.1 h, during anaerobic and aerobic growth, respectively. Doubling times of the FrdB $Val^{207}Cys$ mutant were 4.6 and 3.0 h, respectively, indicating that the mutant enzyme still functions as a bifunctional oxidoreductase and is only partially impaired in the ability to support growth compared to the wild-type enzyme. Also shown in Table II are growth studies for the FrdB $Cys^{204}Ser$, $Cys^{210}Ser$, and $Cys^{214}Ser$ mutants and for the soluble fumarate reductase (FrdAB) which maintains all three iron–sulfur clusters of the enzyme but lacks the FrdCD polypeptides that act as membrane anchors and are necessary for interaction with quinones

(Lemire et al., 1982; Cecchini et al., 1986a; Morningstar et al., 1985). As is the case for the FrdAB enzyme, the FrdB $Cys^{204}Ser$, $Cys^{210}Ser$, and $Cys^{214}Ser$ mutant enzymes are found in the cytoplasmic fraction and hence are incapable of supporting growth on either medium because of the resulting loss of ability to oxidize or reduce bound quinones (Manodori et al., 1991). The effect of these amino acid substitutions on growth is specific for growth on glycerol/fumarate or succinate selective media as evidenced by the normal ability of cells to grow on nonselective glycerol/nitrate or glucose/fumarate media (data not shown).

Enzyme Activity Studies. The catalytic properties of mutant fumarate reductases and wild-type enzyme are also shown in Table II. The values shown reflect both the fumarate reductase activity as measured by oxidation of reduced benzyl viologen or menaquinol and succinate dehydrogenase activity determined by the reduction of PMS or the ubiquinone analogue DPB. Turnover numbers for the FrdB $Cys^{204}Ser$, $Cys^{210}Ser$, and $Cys^{214}Ser$ mutants, where the enzyme is found in the cytoplasmic fraction, show that the enzyme has very little activity in any of the catalytic assays consistent with the loss of one or more Fe–S centers. By comparison, the soluble FrdAB enzyme which contains all three Fe–S clusters (Morningstar et al., 1985) is catalytically competent for fumarate reduction and succinate oxidation. It has, however, lost the ability to interact with quinones, which is consistent with previous studies (Cecchini et al., 1986a; Morningstar et al., 1985). In contrast, the FrdB $Val^{207}Cys$ mutant retains significant catalytic activity in all assays although there is a much greater impairment of the ability of the enzyme to interact with quinones than on interactions with artificial electron donors/acceptors. This latter observation is consistent with an alteration in the properties of the [3Fe–4S] cluster, center 3, which is considered to be the direct donor of electrons to quinone in succinate dehydrogenase (Johnson et al., 1985b; Ohnishi et al., 1976; Beinert et al., 1977). The pronounced reduction in quinone activity of the FrdB $Val^{207}Cys$ mutant could result from dissociation of the catalytic FrdAB subunits from the membrane. To explore this possibility, we measured the amount of covalently bound flavin in the cytoplasmic and membrane fraction of cells grown to log phase in anaerobic glycerol/fumarate medium. The mutation had no discernable effect on the assembly of the fumarate reductase in vivo, as evidenced by identical distributions of covalent FAD found in the membrane and cytoplasmic fractions of mutant cells and wild-type controls. This is in contrast to the FrdB $Cys^{204}Ser$, $Cys^{210}Ser$, and $Cys^{214}Ser$ mutant enzymes, where more than 95% of the enzyme is found in the cytoplasmic fraction of the cells rather than the normal ratio of 75–80% of the enzyme in the membrane-bound form (data not shown).

EPR Studies of the $Cys^{204}Ser$, $Cys^{210}Ser$, and $Cys^{214}Ser$ Mutants. Figure 2 shows EPR spectra for cytoplasmic fractions of DW35 with amplified expression of the FrdB $Cys^{210}Ser$ mutant after oxidation with ferricyanide and reduction with succinate and dithionite. Almost identical spectra were obtained for cytoplasmic fractions of the FrdB $Cys^{204}Ser$ and $Cys^{214}Ser$ mutants (data not shown). For comparison, Figure 3 (left panel) and Figure 4 (upper spectra) show the EPR signals in equivalent redox states for cytoplasmic-membrane preparations of DW35 with amplified expression of wild-type fumarate reductase. Although the characteristic EPR spectrum of the reduced $[2Fe–2S]^+$ cluster, center 1, g = 2.025, 1.930, and 1.920, is clearly present in the succinate- and dithionite-reduced samples of the FrdB $Cys^{204}Ser$, $Cys^{210}Ser$, and $Cys^{214}Ser$ mutants, the rapidly relaxing EPR signal associated with the oxidized $[3Fe–4S]^+$ cluster, center 3, g = 2.016, ~1.98, and ~1.93 (observable at temperatures <30 K), is not seen in ferricyanide-oxidized samples. Rather the spectra comprise only a FAD semiquinone radical signal centered at g = 2.003 that is still observable at temperatures >100 K. Only minimal oxidation compared to the succinate-reduced sample was observed for samples treated with 20 mM fumarate, as judged by the intensity of the EPR signal from reduced center 1.

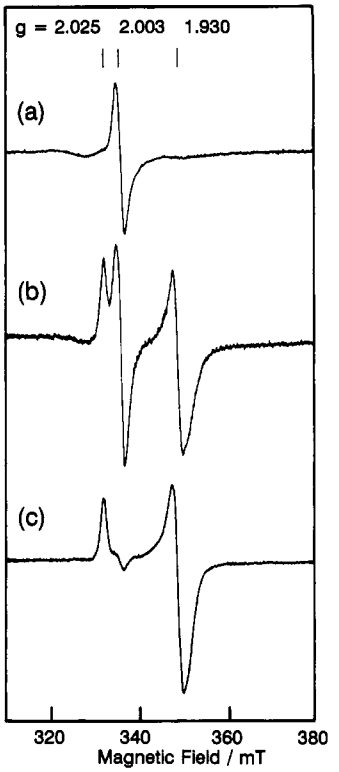

FIGURE 2: EPR spectra of cytoplasmic fractions of *E. coli* DW35 with amplified expression of the $FrdAB^{C210S}CD$ (FrdB $Cys^{210}Ser$ mutant). (a) Oxidized with 5 mM ferricyanide; spectrometer gain = 1.0×10^6, temperature = 10 K. (b) Reduced with 20 mM succinate; spectrometer gain = 4.0×10^6, temperature = 19 K. (c) Reduced with 10 mM dithionite; spectrometer gain = 1.0×10^6, temperature = 19 K. Spectra were recorded at 9.42 GHz with a modulation amplitude of 10 G and a microwave power of 1 mW.

There was also no evidence for a reduced $[4Fe–4S]^+$ cluster, center 2, in dithionite reduced samples of the FrdB $Cys^{204}Ser$, $Cys^{210}Ser$, and $Cys^{214}Ser$ mutants. The presence of center 2 in wild-type fumarate reductase is manifest in two ways. First, it is usually observable as a rapidly relaxing, broad resonance that is apparent at high spectrometer gains to the low and high field of the resonance from center 1 in dithionite-reduced samples (see Figure 4) (Johnson et al., 1985d; Cammack et al., 1986b). No such features were observed in the EPR spectra of the dithionite-reduced samples of these mutants. Second, its presence may be indirectly observed by marked enhancement of the spin relaxation of center 1 in dithionite-reduced compared to succinate-reduced samples. This results from spin–spin interaction between the reduced center 2 ($S = {}^1/_2$, reduced by dithionite but not succinate) and reduced center 1 ($S = {}^1/_2$, partially reduced by succinate) (Morningstar et al., 1985; Johnson et al., 1985d; Cammack et al., 1986b). The power required for half-saturation of an EPR resonance ($P_{1/2}$ value) provides a convenient comparative estimate of spin relaxation rates (the larger the $P_{1/2}$ value the more rapid the spin relaxation). $P_{1/2}$ values for the succinate- and dithionite-reduced forms of the wild-type and mutant enzymes

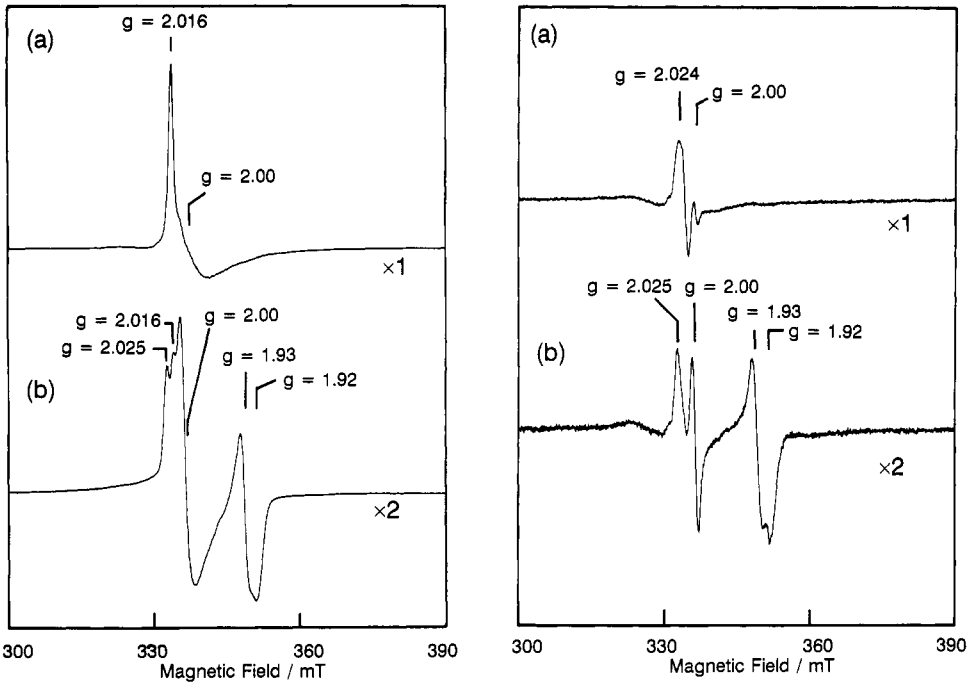

FIGURE 3: EPR spectra of fumarate-oxidized and succinate-reduced cytoplasmic-membrane preparations of *E. coli* DW35 with amplified expression of FrdABCD (wild-type) and FrdAB^{V207C}CD (FrdB Val^{207}Cys mutant). (a) Oxidized with 20 mM fumarate. (b) Reduced with 20 mM succinate. Spectra were recorded at 9.42 GHz with modulation amplitude = 10 G, microwave power = 1 mW, and temperature = 10 K. The multiplication factors indicate the relative spectrometer gains for the spectra of each sample.

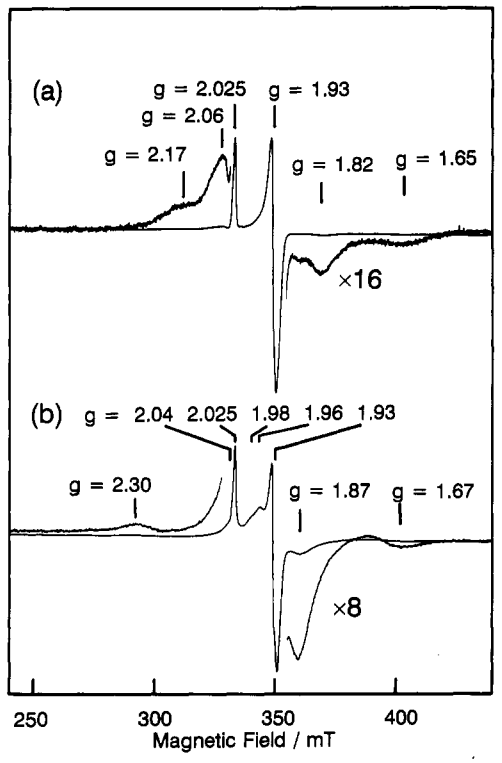

FIGURE 4: EPR spectra of dithionite-reduced cytoplasmic-membrane preparations of *E. coli* DW35 with amplified expression of FrdABCD (wild-type) and FrdAB^{V207C}CD (FrdB Val^{207}Cys mutant). Samples were reduced with 10 mM dithionite. EPR instrument conditions were as described in the legend to Figure 3. The multiplication factors indicate the expansion factors for the expanded regions in each spectra.

investigated in this work are given in Table III. While the wild-type enzyme exhibits a 300-fold increase in the center 1 $P_{1/2}$ value for dithionite- versus succinate-reduced samples, no significant increase was observed for the FrdB Cys^{204}Ser, Cys^{210}Ser and Cys^{214}Ser mutants. These results indicate that neither the [4Fe–4S] cluster, center 2, or the [3Fe–4S] cluster,

Table III: EPR Half-Saturation Powers ($P_{1/2}$ values) at 10 K for Reduced Center 1 in *E. coli* DW35 with Amplified Expression of Wild-Type and Mutant Fumarate Reductase

encoded subunits	$P_{1/2}$ values (mW)	
	succinate-reduced	dithionite-reduced
FrdABCD (wild-type)	0.35	100
FrdAB^{V207C}CD	0.07	41
FrdAB^{C204S}CD	0.07	0.09
FrdAB^{C210S}CD	0.10	0.10
FrdAB^{C214S}CD	0.05	0.07

center 3, are assembled in these cytoplasmic mutant forms of fumarate reductase.

EPR Studies of the Val^{207}Cys Mutant. Figure 3 and 4 compare EPR spectra for cytoplasmic-membrane preparations of DW35 with amplified expression of wild-type and the FrdB Val^{207}Cys mutant after oxidation with fumarate and reduction with succinate and dithionite. In accord with the significant levels of fumarate reductase activity, the addition of fumarate to the cytoplasmic-membrane preparations of the Val^{207}Cys mutant results in oxidation as judged by the loss of the reduced center 1 EPR signal. However, the characteristic resonance of the oxidized [3Fe–4S]$^{+}$ cluster, center 3, was not observed in either fumarate- or ferricyanide-oxidized samples. A weak isotopic resonance centered at $g = 2.02$ was observed, in addition to a radical signal centered at $g = 2.00$, but analogous signals are observed in oxidized cytoplasmic-membrane preparations of the DW35 deletion strain and hence do not arise from the mutant fumarate reductase. Succinate effects only partial reduction of centers 1 and 3 in the wild-type membrane preparations, giving a complicated EPR spectrum comprising overlapping resonances from oxidized center 3, reduced center 1, and the FAD semiquinone radical, whereas only the latter two resonances were observed in succinate-reduced Val^{207}Cys mutant. Previous EPR redox titrations of the herotetrameric *E. coli* fumarate reductase complex have provided evidence for spin–spin interaction between center 1 and center 3 by showing changes in the relaxation properties

of reduced center 1 that occur concomitant with the reduction of center 3 (Cammack et al., 1986b). Although a $[3Fe–4S]^{+,0}$ cluster is paramagnetic in both the oxidized ($S = {}^1/_2$) and reduced ($S = 2$) states, it appears to be more effective in relaxing the spin of reduced center 1 in the oxidized form. Hence, the 5-fold decrease in the $P_{1/2}$ value for center 1 in the succinate-reduced $Val^{207}Cys$ mutant compared to the wild-type (see Table 3) is also consistent with the absence of a $[3Fe–4S]^{+,0}$ cluster in this mutant.

The dithionite-reduced cytoplasmic-membrane preparations of DW35 with amplified expression of wild-type fumarate reductase exhibit the $S = {}^1/_2$ resonance of reduced center 1 and the broad underlying resonance of the $S = {}^1/_2$ reduced $[4Fe–4S]^+$ cluster, center 2, i.e., low-field maxima at $g = 2.17$ and 2.06 and high-field minima at $g = 1.82$ and 1.65, observed only at temperatures below 20 K (Morningstar et al., 1985; Cammack et al., 1986b). While the reduced center 1 EPR signal is also observed in the dithionite-reduced $Val^{207}Cys$ mutant, the form of the broad underlying resonance is quite different with low-field maxima at $g = 2.30$, 2.04 (shoulder), 1.98, and 1.96 and high-field minima at $g = 1.87$ and 1.67 (see Figure 4). Previous EPR studies of the tetrameric complex and dimeric soluble forms of *E. coli* fumarate reductase have shown that complete reduction of center 1 is effected by dithionite, since quantitation of the $g = 2.025$, 1.930, and 1.920 resonance at temperatures between 30 and 70 K accounts for approximately one spin/FAD (Morningstar et al., 1985; Johnson et al., 1985d). Hence the spin concentration of the center 1 EPR resonance over a limited field range of 40 K versus 1 mM CuEDTA standard was used to assess the enzyme concentration of individual samples. Spin quantitation of the entire resonance in the $S = {}^1/_2$ region under nonsaturating conditions (10 K and 50 μW) against a 1 mM CuEDTA standard gave 2.7 spins/molecule for the $Val^{207}Cys$ mutant and 1.8 spins/molecule for the wild-type. Therefore, the broad underlying resonance accounts for ~2 spins/molecule in the $Val^{207}Cys$ mutant compared to ~1 spin/molecule in the wild-type. This indicates the presence of two dithionite-reducible Fe–S clusters that have $S = 0$ and $S = {}^1/_2$ ground states in their oxidized and reduced forms, respectively. Such ground-state properties, coupled with the arrangement of cysteine residues in the mutant FrdB polypeptide, are consistent with the presence of two $[4Fe–4S]^{2+,+}$ clusters, indicating that center 3 is a [4Fe–4S] cluster rather than a [3Fe–4S] cluster in the $Val^{207}Cys$ mutant. The complex broad underlying resonance is, therefore, attributed to spin–spin interaction between the two $S = {}^1/_2$ $[4Fe–4S]^+$, and similar resonances are observed for reduced 8Fe ferredoxins (Mathews et al., 1974). Evidence for spin–spin interaction between reduced center 1 and one or both of these $S = {}^1/_2$ $[4Fe–4S]^+$ clusters comes from the marked enhancement in the spin relaxation (500-fold increase in the $P_{1/2}$ value; see Table III) that accompanies dithionite reduction.

To investigate further the nature of the intercluster spin–spin interactions and the redox potentials of the Fe–S clusters in the $Val^{207}Cys$ mutant, EPR-monitored redox titrations were undertaken. Only the results of oxidative titrations are presented below, however, analogous results without any significant hysteresis were observed in subsequent reductive titrations. The midpoint potential of center 1 was unchanged relative to the wild-type membranes ($E_m = -79$ mV; Werth et al., 1990). Figure 5 shows EPR spectra at 10 K and 1-mW microwave power for the $Val^{207}Cys$ mutant membranes poised at −190, −290, and −425 mV (vs NHE). The EPR signal from reduced center 1 is already fully developed at −190 mV, and

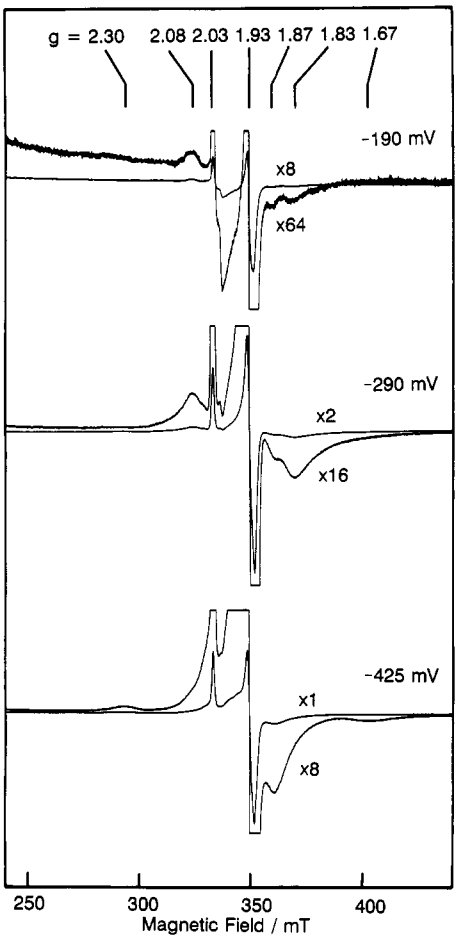

FIGURE 5: EPR spectra of cytoplasmic-membrane preparations of *E. coli* DW35 with amplified expression of $FrdAB^{V207C}CD$ (FrdB $Val^{207}Cys$ mutant) poised at selected redox potentials. Samples were poised at the indicated potential (vs NHE) as described under Materials and Methods. Spectra were recorded at 9.42 GHz with modulation amplitude = 10 G, microwave power = 10 mW, and temperature = 10 K. The multiplication factors indicate the relative spectrometer gains for all spectra.

the apparent increase in intensity of this resonance at lower potentials is a consequence of relief of saturation resulting from relaxation enhancement via spin–spin interaction with the lower potential $S = {}^1/_2$ $[4Fe–4S]^+$ clusters. Starting at about −190 mV, a broad underlying resonance with a low-field maxima at $g = 2.08$ and a high-field minima at $g = 1.83$ starts to grow in as the potential is decreased, reaching a maximum at ~−290 mV. These features then begin to decrease with a concomitant increase of the more complex features observed in the dithionite-reduced samples. Such behavior is consistent with the presence of two low-potential $[4Fe–4S]^{2+,+}$ clusters, with the $g = 2.08$ and 1.83 features resulting from the reduction of the higher potential cluster (A) and the more complex resonance arising from spin coupling between the pair of reduced clusters (A + B). The redox potentials of each cluster were assessed by Gaussian deconvolution of the $g = 1.87$ and 1.83 features which are proportional to the concentrations of reduced (A + B) and reduced A, respectively, and plotting their intensities as a function of potential (see Figure 6). Analysis of the data assumed that the interaction between the reduced clusters is sufficient to alter their EPR properties but not their redox behavior, as is the case in 8Fe ferredoxins (Mathews et al., 1974; Prince & Adams, 1987), and followed that described in Makund and Adams (1990). The theoretical curves are constructed for one-electron reduction of A and B with $E_{mA} = -240$ mV and $E_{mB} = -350$ mV.[2] The concen-

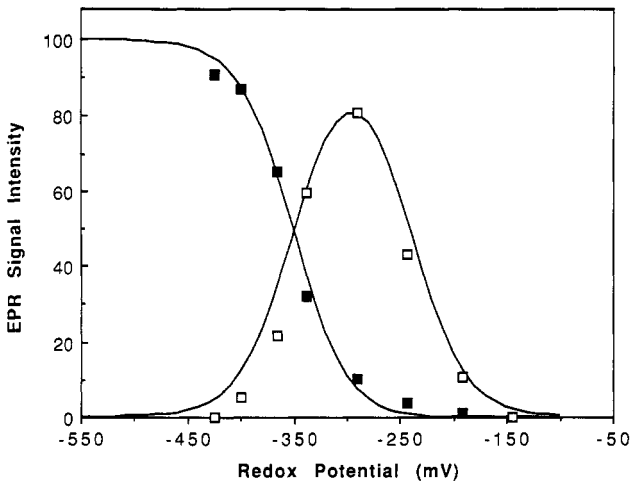

FIGURE 6: Redox behavior of the $[4Fe–4S]^{2+,+}$ clusters in cytoplasmic-membrane preparations of *E. coli* DW35 with amplified expression of $FrdAB^{V207C}CD$ (FrdB $Val^{207}Cys$ mutant). Redox titrations were carried out as described under Materials and Methods and the conditions for EPR spectroscopy are in the legend to Figure 5. The concentration of reduced cluster A (□) and reduced clusters A + B (■) was assessed by the amplitude of the $g = 1.83$ and 1.87 signals, respectively, after Gaussian deconvolution of these resonances. The theoretical curves are calculated for one-electron reduction of A and B with $E_m = -240$ mV for cluster A and $E_m = -350$ mV for cluster B.

trations of $A_{red}B_{ox}$ and $A_{ox}B_{red}$ reach maxima of 80% and 1%, respectively, at −295 mV.

The assignment of A or B to the indigenous [4Fe–4S] cluster, center 2, or the [4Fe–4S] cluster assembled as center 3 cannot be made with certainty. The midpoint potential of center 2 in membrane-bound preparations, −285 to −300 mV (Simpkin & Ingledew, 1985; Werth et al., 1990), lies between the two potentials, suggesting that it is slightly perturbed in the mutant enzyme. However, the similarity of the EPR signal associated with the higher potential cluster, as seen in the sample poised at −290 mV, to that of center 2 in the wild-type membranes suggests that A corresponds to the indigenous [4Fe–4S] cluster, center 2. The major difference is in the absence of the high- and low-field features of $g = 2.17$ and 1.65, which is understandable since they are most likely a consequence of intercluster spin coupling between the $S = {}^1/_2$ $[4Fe–4S]^+$ and the $S = 2$ $[3Fe–4S]^0$ in the wild-type enzyme (Ohnishi, 1987; Salerno & Yan, 1987; Ackrell et al., 1991). Hence we tentatively assign the higher potential cluster, $E_m = -240$ mV, to center 2, and the lower potential cluster, $E_m = -350$ mV, to the [4Fe–4S] cluster that has been assembled as center 3.

Discussion

The growth properties, enzymatic activities, and EPR studies of the *E. coli* fumarate reductase site-directed mutants reported in this work provide further insight into the roles of the [4Fe–4S] and [3Fe–4S] clusters (centers 2 and 3, respectively) in electron transport through this complex respiratory chain enzyme, the residues involved in ligating these clusters, and the spatial arrangement of all three clusters as revealed by intercluster magnetic interactions. Each of these aspects is discussed separately below. Of particular importance are the results for the $Val^{207}Cys$ mutant which show that the primary structure of an Fe–S protein determines the type of cluster assembled and permit elucidation of the enzymatic consequences associated with changing center 3 from a [3Fe–4S] to a [4Fe–4S] cluster.

The role of [3Fe–4S] clusters in biology is still the subject of much current interest. It is clear that some are artifacts produced by oxidative degradation of [4Fe–4S] clusters during isolation (Beinert & Thomson, 1983). Most recently, the sequence homology between aconitase and the iron-responsive element binding protein has lead to the suggestion that [3Fe–4S] ↔ [4Fe–4S] interconversions may have physiological relevance in regulating intracellular iron by controlling expression of ferritin and transferrin receptors (Rouault et al., 1991). However, in the case of fumarate reductase and succinate dehydrogenase, the available evidence supports the view that the [3Fe–4S] cluster functions in mediating electron transfer to and from bound quinones and is an intrinsic part of the respiratory chain. Previous studies have shown that the EPR signal associated with oxidized center 3 is readily detected in fumarate-treated whole cells of *E. coli* with amplified expression of fumarate reductase (Johnson et al., 1985c) and that facile [3Fe–4S] → [4Fe–4S] cluster conversion does not occur in soluble preparations of mammalian succinate dehydrogenase (Johnson et al., 1985b) or *E. coli* fumarate reductase (Morningstar et al., 1985). In accord with earlier results on the soluble two-subunit enzymes (Johnson et al., 1985b; Morningstar et al., 1985), the studies of the FrdB $Cys^{204}Ser$, $Cys^{210}Ser$, and $Cys^{214}Ser$ mutants reported above demonstrate that assembly of center 3 is necessary for membrane attachment and sustaining electron transport to or from quinones. Moreover, although the EPR studies of the *E. coli* FrdB $Val^{207}Cys$ mutant reported here show that center 3 is assembled as a [4Fe–4S] cluster rather than a [3Fe–4S] cluster when an additional cysteine residue is provided, the resulting membrane-bound enzyme is greatly impaired in its ability to accept electrons from menaquinol, the physiological electron donor.

In addition to fumarate reductases and succinate dehydrogenases, there are now at least two other metalloenzymes that contain [3Fe–4S] clusters which appear, on the basis of amino acid sequence data and spectroscopic studies, to be intrinsic electron transport components of the enzymes in vivo. These are *E. coli* nitrate reductase (Johnson et al., 1985a; Blasco et al., 1989) and spinach glutamate synthase (Knaff et al., 1991). Hence, there seems little remaining doubt than [3Fe–4S] clusters do function in biological electron transport. The choice of a $[3Fe–4S]^{+,0}$ cluster over a $[4Fe–4S]^{2+,+}$ cluster is most likely dictated by a requirement for a higher redox potential, since the midpoint potentials are generally in the range +80 to −250 mV and −300 to −600 mV, for $[3Fe–4S]^{+,0}$ and $[4Fe–4S]^{2+,+}$ clusters, respectively (Ackrell et al., 1991).

The consequences of converting center 3 from a [3Fe–4S] to a [4Fe–4S] cluster via the $Val^{207}Cys$ mutation are a 50% decrease in growth rate and catalytic activity (measured with BV_{red} and PMS) and an even greater decrease (>80%) in the ability to interact with quinones (as measured by activities with MQH_2 and DPB). However, it is evident that the presence of the [3Fe–4S] cluster per se is *not essential* for a functional enzyme. Moreover, it is clear that either a [3Fe–4S] or the [4Fe–4S] cluster provides the scaffold for structural integrity of the enzyme since the enzyme remains membrane bound and is still able to interact with quinones to an extent sufficient

[2] At the suggestion of one of the reviewers, analysis of the EPR redox titration was also conducted using the intensity of the $g = 2.30$ (A + B) and $g = 2.08$ (A) features. The contribution of the A + B resonance at $g = 2.08$ was estimated, on the basis of the intensity ratio at $g = 2.30$ and 2.08 in the most reduced samples, and subtracted at each potential. This analysis yielded best fits with $E_{mA} = -250$ mV and $E_{mB} = -345$ mV (data not shown), in excellent agreement with the values obtained using $g = 1.87$ (A + B) and $g = 1.83$ (A).

to support growth of *E. coli* under conditions requiring a physiologically competent fumarate reductase and/or succinate dehydrogenase. The decrease in growth rate and catalytic activity are most likely related to the decrease in midpoint potential of the modified center 3 from −70 to −350 mV, making electron transfer to or from bound quinones much less thermodynamically favorable. It is possible that menaquinol (E_m = −74 mV; Ingledew & Poole, 1984) directly reduces center 1 (E_m = −79 mV; Werth et al., 1990) in the FrdB $Val^{207}Cys$ mutant using an alternative electron transfer pathway that bypasses center 3. Conceivably these enzymes may have evolved from 8Fe ferredoxins with two low-potential [4Fe–4S] clusters and that during the course of evolution a simple amino acid substitution of valine for cysteine could have formed the higher potential [3Fe–4S] cluster, making the enzyme much more efficient for fumarate reduction and succinate oxidation.

The mutation of each of the last three cysteines to serines in the FrdB subunit implicates Cys^{204}, Cys^{210}, and Cys^{214} as potential ligands for centers 2 or 3. These mutants do not, however, address the question of which specific residues ligate each cluster, since neither cluster is assembled and the resulting cytoplasmic enzyme has little catalytic activity. In contrast, the $Val^{207}Cys$ mutant studies strongly support the assignment that is suggested by analogy to the sequence of structurally characterized bacterial ferredoxins, i.e., Cys^{148}, Cys^{151}, Cys^{154}, and Cys^{214} ligating center 2 and Cys^{158}, Cys^{204}, and Cys^{210} ligating center 3. The fact that the $Val^{207}Cys$ mutation results in assembly of a [4Fe–4S] cluster rather than a [3Fe–4S] cluster is in itself strong support for this assignment. Additional evidence comes from the EPR spectrum of the dithionite-reduced $Val^{207}Cys$ mutant. The broad complex resonance is indicative of spin coupling between two $S = {}^1/_2$ $[4Fe–4S]^+$ clusters and is very similar to the spectra observed for reduced 8Fe ferredoxins which have analogous arrangements of cysteine residues.

Previous EPR studies indicated that center 2, but not center 3, was assembled in cytoplasmic fractions of an *E. coli* FrdABCD deletion strain with amplified expression of FrdAB*, where B* indicates a B subunit truncated between the second and third group of cysteine residues so that Cys^{204}, Cys^{210}, and Cys^{214} were not present (Johnson et al., 1988). The evidence was based solely on enhanced spin relaxation for center 1 in dithionite-compare to succinate-reduced samples, i.e., an EPR signal from reduced center 2 was not observed directly. From this it was concluded that none of the last three cysteines were ligands to center 2 in the wild-type enzyme. In contrast, neither center 2 nor center 3 was assembled in the $Cys^{204}Ser$, $Cys^{210}Ser$, or $Cys^{214}Ser$ site-directed mutants investigated in this work. The only explanation for these apparently contradictory results is that some type of dithionite-reducible Fe–S cluster, related or unrelated to center 2, is assembled in the FrdAB* subunits. For example, it is conceivable that a $[4Fe–4S]^{2+,+}$ is assembled with a water molecule or some other residue occupying the fourth coordination position, as is the case in ferredoxins from *P. furiosus* (Conover et al., 1990) and *D. africanus* (George et al., 1989). The $[4Fe–4S]^+$ clusters in these ferredoxins have predominantly $S = {}^3/_2$ ground states, and it would not be possible to observe EPR resonances from such centers in the dilute cytoplasmic fractions used in the previous work. We are in the process of investigating such possibilities with purified samples of FrdAB*.

The $Val^{207}Cys$ mutant studies support the view that the primary sequence of an Fe–S protein determines the type of cluster inserted. In accord with this, Rothery and Weiner (1991) have recently shown that it is possible to change one of the four [4Fe–4S] clusters of dimethyl sulfoxide reductase to a [3Fe–4S] cluster by changing the amino acid sequence of this protein to mimic the region encoding the [3Fe–4S] cluster of nitrate reductase. The mutation involved changing the second Cys in a ferredoxin-like Cys–xx–Cys–xx–Cys–xxx–Cys–Pro sequence to Trp, Ser, Phe, or Tyr. The resulting cluster had at least a 200-mV rise in midpoint potential, consistent with the lowered redox potential we observe for the [3Fe–4S] to [4Fe–4S] change in fumarate reductase. The modified DMSO reductase, however, was unable to support growth anaerobically under selective conditions, which most likely reflects the inability of the modified cluster, E_m = >+150 mV, to mediate electron transfer from menaquinol to the molybdopterin active site.

The ability to alter the ground-state magnetic properties and lower the midpoint potential of center 3 via the $Val^{207}Cys$ mutation, while maintaining the structural integrity of the enzyme complex, has also permitted a clearer understanding of the EPR spectra and intercluster spin–spin interactions in the wild-type enzyme. In particular, the ability to observe the EPR of reduced center 2 with center 3 as a diamagnetic $[4Fe–4S]^{2+}$ cluster, rather than a paramagnetic $[3Fe–4S]^0$ cluster, provides further evidence that the g = 2.17 and 1.65 features of the center 2 EPR signal in the wild-type enzyme arise from spin–spin interaction with the $S = 2$ $[3Fe–4S]^0$ cluster. Furthermore, EPR redox titrations show that the spin-coupled EPR signal in the dithionite-reduced $Val^{207}Cys$ mutant arises from interaction between centers 2 and 3, indicating they are also close enough for intercluster spin–spin interaction in the mutant enzyme. Hence we conclude that weak intercluster magnetic interactions exist between each pair of clusters in *E. coli* fumarate reductase, suggesting that each is within 8–20 Å of the other two. The interaction between centers 2 and 3 is manifest in terms of perturbation of the center 2 EPR signal, suggesting a much closer spatial proximity compared to centers 1 and 2 or centers 1 and 3, where the interactions are apparent only in terms of relaxation enhancement of center 1. Attempts to simulate the complex spin-coupled EPR spectra in both the wild-type and $Val^{207}Cys$ mutant enzymes are in progress in order to provide a more precise measure of the spatial separation between centers 2 and 3 in these enzymes.

Finally we turn our attention to the implications of these results for the mechanism of electron transport through the Fe–S clusters of fumarate reductases or succinate dehydrogenases. Two distinct proposals have been advanced in the literature to explain the presence of an Fe–S cluster, center 2, with a midpoint potential approximately 250 mV lower than either the succinate/fumarate or Q/QH_2 couples. Cammack et al. (1986a, 1987) proposed a dual pathway model for electron transfer through cardiac complex II which provides for two-step reduction of Q and oxidation of $FADH_2$ by assuming that the low-potential center 2 and cytochrome *b* mediate electron transfer between $Q/QH^\bullet$ and $FADH^\bullet/FAD$ and that centers 1 and 3 provide a higher potential pathway linking $QH^\bullet/QH_2$ and $FADH_2/FADH^\bullet$. The results presented above demonstrate that centers 2 and 3 are spatially in very close proximity. Hence strict channeling of electrons through these two pathways is unlikely since reduction of center 3 by center 2 would short-circuit the low-potential pathway. However, it is possible provided the reaction cycle begins to an odd-electron state which would be regained by the release of $QH^\bullet$ (Cammack et al., 1987). Under such

conditions, the high-potential centers would always be reduced *before* the low-potential centers.

The problem with the dual pathway model is that the low-potential one-electron couples of $FADH^{\bullet}/FADH_2$ and $QH^{\bullet}/QH_2$ (ubiquinone or menaquinone) are more nearly isopotential with the succinate-reducible high-potential clusters, centers 1 and 3, than the low-potential cluster, center 2 (Salerno, 1991). Indeed, this observation has lead to an alternative proposal (Salerno, 1991) involving a linear sequence of sequential one-electron transfers, center 1 ↔ center 2 ↔ center 3, with center 1 interacting with FAD, $FADH^{\bullet}$, and $FADH_2$ and center 3 interacting with Q, $QH^{\bullet}$, and QH_2. Central to this proposal is that the midpoint potential of center 2, as measured by equilibrium redox titrations, is an apparent potential that is lower than the intrinsic potential by approximately 250 mV as a result of anticooperative redox interactions between centers 1 and 2 and centers 2 and 3. While these interactions favor separation of electrons under equilibrium conditions, transient electron transfer through the intermediate cluster, center 2, could be energetically feasible at lower levels of reduction. However, this work and our previous studies of mutations in the residues ligating center 1 argue strongly that the intrinsic midpoint potential of center 2 is <–240 mV, since its potential as measured in equilibrium redox titrations is not dramatically altered on lowering the potential of either center 1 by 250 mV (Werth et al., 1990) or center 3 by 280 mV (this work).

The results presented here suggest an alternative proposal, namely, that center 2 is a vestige of the evolution of Ip subunits from an 8Fe ferredoxin and that, while it is necessary for structural integrity and membrane binding of the enzyme, it does not function directly in electron transfer between the covalently FAD and quinone. Hence, we currently favor a linear electron transfer pathway through the Fe–S clusters of fumarate reductase and succinate dehydrogenase involving only centers 1 and 3. While this pathway is optimal, alternative pathways that bypass either center 1 or center 3 become operative if the potential of either cluster is dramatically decreased while preserving the overall structural integrity of the enzyme complex. These alternative pathways result in functional albeit much less efficient enzymes.

ACKNOWLEDGMENTS

We thank Dr. Michael W. W. Adams for assistance in analyzing the EPR redox titration data and Dr. Brian A. C. Ackrell for many stimulating discussions.

REFERENCES

Ackrell, B. A. C., Johnson, M. K., Gunsalus, R. P., & Cecchini, G. (1991) in *Chemistry and Biochemistry of Flavoenzymes* (Muller, F., Ed.) Vol. III, pp 229–297, CRC Press, Boca Raton, FL.

Adman, E. T., Sieker, L. C., & Jensen, L. H. (1973) *J. Biol. Chem. 248*, 3987–3996.

Beinert, H., & Thomson, A. J. (1983) *Arch. Biochem. Biophys. 222*, 333–361.

Beinert, H., Ackrell, B. A. C., Vinogradov, A. D., Kearney, E. B., & Singer, T. P. (1977) *Arch. Biochem. Biophys. 182*, 95–106.

Blasco, F., Iobbi, C., Giordano, G., Chippaux, M., & Bonnefoy, V. (1989) *Mol. Gen. Genet. 218*, 249–256.

Blaut, M., Whittaker, K., Valdovinos, A., Ackrell, B. A. C., Gunsalus, R. P., & Cecchini, G. (1989) *J. Biol. Chem. 264*, 13599–13604.

Cammack, R., Crowe, B. A., & Cook, N. B. (1986a) *Biochem. Soc. Trans. 14*, 1207–1212.

Cammack, R., Patil, D. S., & Weiner, J. H. (1986b) *Biochim. Biophys. Acta 870*, 545–551.

Cammack, R., Maguire, J. J., & Ackrell, B. A. C. (1987) in *Cytochrome Systems: Molecular Biology and Bioenergetics* (Papa, S., Chance, B., & Ernster, L., Eds.) pp 485–491, Plenum Press, New York.

Cecchini, G., Ackrell, B. A. C., Deshler, J. O., & Gunsalus, R. P. (1986a) *J. Biol. Chem. 261*, 1808–1814.

Cecchini, G., Thompson, C. R., Ackrell, B. A. C., Westenberg, D. J., Dean, N., & Gunsalus, R. P. (1986b) *Proc. Natl. Acad. Sci. U.S.A. 83*, 8898–8902.

Cole, S. T., Grundström, T., Jaurin, B., Robinson, J. J., & Weiner, J. H. (1982) *Eur. J. Biochem. 126*, 211–216.

Cole, S. T., Condon, C., Lemire, B. D., & Weiner, J. H. (1985) *Biochim. Biophys. Acta 811*, 381–403.

Conover, R. C., Kowal, A. T., Fu, W., Park, J.-B., Aono, S., Adams, M. W. W., & Johnson, M. K. (1990) *J. Biol. Chem. 265*, 8533–8541.

Darlison, M. G., & Guest, J. R. (1984) *Biochem. J. 223*, 507–517.

George, S. J., Armstrong, F. A., Hatchikian, E. C., & Thomson, A. J. (1989) *Biochem. J. 264*, 275–284.

Guest, J. R. (1981) *J. Gen. Microbiol. 122*, 171–179.

Hanahan, D. (1983) *J. Mol. Biol. 166*, 557–580.

Howard, J. B., Lorsbach, T. W., Ghosh, D., Melis, K., & Stout, C. D. (1983) *J. Biol. Chem. 258*, 508–522.

Ingledew, W. J., & Poole, R. K. (1984) *Microbiol. Rev. 48*, 222–271.

Johnson, M. K., Bennett, D. E., Morningstar, J. E., Adams, M. W. W., & Mortenson, L. E. (1985a) *J. Biol. Chem. 260*, 5456–5463.

Johnson, M. K., Morningstar, J. E., Bennett, D. E., Ackrell, B. A. C., & Kearney, E. B. (1985b) *J. Biol. Chem. 260*, 7368–7378.

Johnson, M. K., Morningstar, J. E., Cecchini, G., & Ackrell, B. A. C. (1985c) *Biochem. Biophys. Res. Commun. 131*, 653–658.

Johnson, M. K., Morningstar, J. E., Cecchini, G., & Ackrell, B. A. C. (1985d) *Biochem. Biophys. Res. Commun. 131*, 756–762.

Johnson, M. K., Kowal, A. T., Morningstar, J. E., Oliver, M. E., Whittaker, K., Gunsalus, R. P., Ackrell, B. A. C., & Cecchini, G. (1988) *J. Biol. Chem. 263*, 14732–14738.

Joyce, C. M., & Grindley, N. D. F. (1984) *J. Bacteriol. 158*, 636–643.

Kissinger, C. R., Adman, E. T., Sieker, L. C., & Jensen, L. H. (1988) *J. Am. Chem. Soc. 110*, 8721–8723.

Kissinger, C. R., Adman, E. T., Sieker, L. C., Jensen, L. H., & LeGall, J. (1989) *FEBS Lett. 244*, 447–450.

Knaff, D. B., Hirasawa, M., Ameyibor, E., Fu, W., & Johnson, M. K. (1991) *J. Biol. Chem. 266*, 15080–15084.

Kröger, A. (1978) *Biochim. Biophys. Acta 505*, 129–145.

Kunkel, T. A. (1985) *Proc. Natl. Acad. Sci. U.S.A. 82*, 488–492.

Kunkel, T. A., Roberts, J. D., & Zakour, R. A. (1987) *Methods Enzymol. 154*, 367–382.

Lauterbach, F., Körtner, C., Albracht, S. P. J., Unden, G., & Kröger, A. (1990) *Arch. Microbiol. 154*, 386–393.

Lemire, B. D., & Weiner, J. H. (1986) *Methods Enzymol. 126*, 377–386.

Lemire, B. D., Robinson, J. J., & Weiner, J. H. (1982) *J. Bacteriol. 152*, 1126–1131.

Manodori, A., Cecchini, G., Werth, M. T., Johnson, M. K., Schröder, I., & Gunsalus, R. P. (1991) in *Flavins and Flavoproteins 1990* (Curti, B., Roncho, S., & Zanetti, G.,

Eds.) pp 719-722, Walter de Gruyter, Berlin.
Mathews, R., Charlton, S., Sands, R. H., & Palmer, G. (1974) *J. Biol. Chem. 249*, 4326-4328.
Messing, J., & Vieira, J. (1982) *Gene 19*, 269-276.
Morningstar, J. E., Johnson, M. K., Cecchini, G., Ackrell, B. A. C., & Kearney, E. B. (1985) *J. Biol. Chem. 260*, 13631-13638.
Mukund, S., & Adams, M. W. W. (1990) *J. Biol. Chem. 265*, 11508-11516.
Ohnishi, T. (1987) *Curr. Top. Bioenerg. 15*, 37-65.
Ohnishi, T., Lim, J., Winter, D. B., & King, T. E. (1976) *J. Biol. Chem. 251*, 2105-2109.
Phillips, M. K., Hederstedt, L., Hasnain, S., Rutberg, L., & Guest, J. R. (1987) *J. Bacteriol. 169*, 864-873.
Prince, R. C., & Adams, M. W. W. (1987) *J. Biol. Chem. 262*, 5125-5128.
Rothery, R. A., & Weiner, J. H. (1991) *Biochemistry 30*, 8296-8305.
Rouault, T. C., Stout, C. D., Kaptain, S., Harford, J. B., & Klausner, R. D. (1991) *Cell 64*, 881-883.
Salach, J., Walker, W. H., Singer, T. P., Ehrenberg, A., Hemmerich, P., Ghisla, S., & Hartmann, U. (1972) *Eur. J. Biochem. 26*, 267-278.
Salerno, J. C., & Yan, X. (1987) in *Cytochrome Systems: Molecular Biology and Bioenergetics* (Papa, S., Chance, B., & Ernster, L., Eds.) pp 467-471, Plenum Press, New York.
Sanger, F., Nicklen, S., & Coulson, A. R. (1977) *Proc. Natl. Acad. Sci. U.S.A. 74*, 5463-5467.
Sato, S., Nakazawa, K., Hon-nami, K., & Oshima, T. (1981) *Biochim. Biophys. Acta 668*, 277-289.
Schröder, I., Gunsalus, R. P., Ackrell, B. A. C., Cochran, B., & Cecchini, G. (1991) *J. Biol. Chem. 266*, 13572-13579.
Simpkin, D., & Ingledew, W. J. (1980) *Biochem. Soc. Trans. 13*, 602-607.
Weiner, J. H., & Dickie, P. (1979) *J. Biol. Chem. 154*, 8590-8593.
Werth, M. T., Cecchini, G., Manodori, A. M., Ackrell, B. A. C., Schröder, I., Gunsalus, R. P., & Johnson, M. K. (1990) *Proc. Natl. Acad. Sci. U.S.A. 87*, 8965-8969.
Yao, Y., Wakabayashi, S., Matsubara, H., Yu, L., & Yu, C.-A. (1986) in *Iron-Sulfur Protein Research* (Matsubara, H., Katsube, Y., & Wada, K., Eds.) pp 240-244, Japan Science Society Press, Tokyo.

Inorganic Phosphate Binding and Electrostatic Effects in the Active Center of Aspartate Aminotransferase Apoenzyme†

Jose H. Martinez-Liarte,‡ Ana Iriarte, and Marino Martinez-Carrion*
School of Basic Life Sciences, University of Missouri—Kansas City, BSB 109, Kansas City, Missouri 64110-2499
Received September 18, 1991; Revised Manuscript Received December 23, 1991

ABSTRACT: The ionization state of the phosphate group bound at the aspartate aminotransferase apoenzyme's active site has been investigated utilizing Fourier-transform infrared spectroscopy following the band corresponding to the symmetric stretching of the dianionic phosphate. Unlike free phosphate, when inorganic phosphate is bound at the enzyme's active site, the integrated intensity value of the dianionic band does not change with pH within the studied range, and this value is similar to that for free dianionic phosphate at pH 8.3. From these results, we propose a dianionic state for the phosphate ion bound to cytosolic aspartate aminotransferase throughout the pH range of 5.7-8.3. The presence of other anions such as acetate and chloride or the substrate aspartate and its analogues produces a pH-dependent phosphate removal from the active site which is favored at low pH values. Elimination of the charged primary amine at the active-site Lys-258, through formation of a Schiff base with pyridoxal or chemical modification by carbamylation, also produces a pH-independent phosphate release. These results are interpreted as Lys-258 together with the active-site α-helix and other residues may be involved in stabilizing phosphate as a dianion in the apoenzyme phosphate pocket which anchors the phosphate ester of pyridoxal phosphate in the holoenzyme. It is proposed that the dianionic phosphate contributes to the apoenzyme's thermal stability through formation of strong hydrogen bond and salt bridges with the amino acid residues forming the phosphate binding pocket with assistance of Lys-258, and other active-site cationic components.

Aspartate aminotransferase (EC 2.6.1.1) is a dimeric enzyme composed of identical subunits with each active site containing pyridoxal 5′-phosphate (PLP) linked via an internal Schiff base to a lysine residue. This enzyme exists as two isozymes with different locations in the cell: mitochondria and cytosol. The apoenzyme forms of these isozymes are also known to bind ions at the active site where they both act as competitive inhibitors (Jenkins & D'Ari, 1966b; Martinez-Carrion et al., 1973; Cheng & Martinez-Carrion, 1972; Martinez-Carrion, 1985) and prevent binding of the coenzyme pyridoxal or pyridoxamine phosphate. In addition, phosphate ions induce both stabilization of this enzyme toward thermal denaturation (Iriarte et al., 1985) and resistance to proteolytic attack (Iriarte et al., 1984). Yet, little is known regarding the forces involved in the binding of ions including phosphate.

Fourier-transform infrared (FTIR) spectroscopy has been recently used by us to study the ionization state of the phosphate group in PLP in both cytosolic and mitochondrial aspartate aminotransferases (Sanchez-Ruiz & Martinez-Carrion,

† This work was supported by Grants GM-38341 and HL-38412 from the National Institutes of Health.
‡ Present address: Departamento de Bioquímica y Biología Molecular, Facultad de Medicina, Universidad de Murcia, 30100 Murcia, Spain.

0006-2960/92/0431-2712$03.00/0